Synergetic measurements of aerosols over São Paulo, Brazil using LIDAR, sunphotometer and satellite data during the dry season

E. Landulfo, A. Papayannis, P. Artaxo, A. D. A. Castanho, A. Z. de Freitas, R. F. Sousa, N. D. Vieira Junior, M. P. M. P. Jorge, O. R. Sánchez-Ccoyllo, D. S. Moreira

Atmos. Chem. Phys. Discuss., 3, 2835–2877, 2003
www.atmos-chem-phys.org/acpd/3/2835/

Atmospheric Chemistry and Physics Discussions

Synergetic measurements of aerosols over São Paulo, Brazil using LIDAR, sunphotometer and satellite data during the dry season

E. Landulfo[1], A. Papayannis[2], P. Artaxo[3], A. D. A. Castanho[3], A. Z. de Freitas[1], R. F. Sousa[1], N. D. Vieira Junior[1], M. P. M. P. Jorge[4], O. R. Sánchez-Ccoyllo[5], and D. S. Moreira[5]

[1]Instituto de Pesquisas Energéticas e Nucleares, São Paulo, Brazil
[2]National Technical University of Athens, Athens, Greece
[3]Instituto de Fisica da Universidade de São Paulo, São Paulo, Brazil
[4]Instituto de Nacional de Pesquisas Espaciais, São José dos Campos, Brazil
[5]Instituto de Geofisica, Astronomia e Ciências Atmosféricas da Universidade de São Paulo, São Paulo, Brazil

Received: 30 April 2003 – Accepted: 15 May 2003 – Published: 2 June 2003

Correspondence to: E. Landulfo (elandulf@net.ipen.br)

Abstract

A backscattering LIDAR system, the first of this kind in Brazil, has been set-up in a suburban area in the city of São Paulo (23°33′ S, 46°44′ W) to provide the vertical profile of the aerosol backscatter coefficient at 532 nm up to an altitude of 4–6 km above sea level (a.s.l.). The measurements have been carried out during the second half of the so-called Brazilian dry season, September and October 2001 and during the first half of the dry season in August and September 2002. The LIDAR data are presented and analysed in synergy with aerosol optical thickness (AOT) measurements obtained by a CIMEL sun-tracking photometer in the visible spectral region and with satellite measurements obtained by the MODIS sensor. This synergetic approach has been used, not only to validate the LIDAR data, but also to derive a typical value (45 sr) of the so-called extinction-to-backscatter ratio (LIDAR ratio) during the dry season. The satellite data analysis offers additional information on the spatial distribution of aerosols over Brazil including the determination of aerosol source regions over the country. The LIDAR data were also used to retrieve the Planetary Boundary Layer (PBL) height, aerosol layering and the structure of the lower troposphere over the city of São Paulo. These first LIDAR measurements over the city of São Paulo during the dry season showed a significant variability of the AOT in the lower troposphere (0.5–5 km) at 532 nm. It was also found that the aerosol load is maximized in the 1–3 km height region, although up to 3 km thick aerosol layers were also detected in the 2.5–5.5 km region in certain cases. Three-dimensional 96-hours air mass back-trajectory analysis was also performed in selected cases to determine the source regions of aerosols around São Paulo during the dry season.

1. Introduction

Suspended aerosol particles play a significant role in Global Change issues, since they influence the earth's radiation balance and climate by scattering or absorbing both

ACPD

3, 2835–2877, 2003

incoming and outgoing radiation and by acting as cloud condensation nuclei (CCN). Tropospheric aerosols arise from natural sources, such as airborne dust, sea-spray and volcanoes and also from anthropogenic sources, such as combustion of fossil fuels and biomass burning activities and from gas-to-particles conversion processes (Pandis et al., 1995).

Air pollution in mega cities is one of the most important problems of our era. São Paulo is among the five largest metropolitan areas of the world, as well as one of the most populated with about 10 million inhabitants. Therefore, in all these mega-cities the human activities have an enormous impact on the air quality, as well as on their population health (Saldiva et al., 1995). Concerning the atmospheric quality, we highlight the suspended aerosol particles as a subject of continuous interest due the on-going expansion of the São Paulo metropolitan area, which carries more than 3.000 industries. Among them the main aerosol sources include heavy industries, such as iron and steel works, refineries, chemical manufacturing, cement, sulphuric acid, petrochemical plants and the automotive fleet, exceeding already 5 million vehicles.

Regarding its topography the city of São Paulo is located in a plateau at about 800 m a.s.l. and is surrounded by mountains of about 1200 m height. During the summer season the precipitation increases and many cold fronts generate meteorological instabilities which indeed favour the pollution dispersion. These periods can extend over the autumn months of May and June, further on when the wintertime begins, a high pressure semi-static regime over the São Paulo area is generally observed. This event becomes highly favourable to air pollutants accumulation, especially during episodes of intense temperature inversions, occurring typically at 1000 m a.s.l. (Alonso et al., 1999).

In this study in addition to local urban pollution, we also searched for potential sources of biomass burning (pyrogenic) aerosols, due to clear forest activities in the Amazon basin and harvesting areas in neighbouring regions and also in the north western-central Brazil during the dry season. These aerosols can be transported over the city of São Paulo, even from more remote areas, especially in September, when

ACPD
3, 2835–2877, 2003

the biomass burning activities peak in central Brazil.

To study this biomass burning aerosols over the city of São Paulo we applied a strategy like the multi-platform campaign called INDOEX (Indian Ocean Experiment), which was organized to measure the long-range transport of air pollution from South and Southeast Asia toward the Indian Ocean during the dry monsoon season, where biomass burning activities are maximized (Lelieveld et al., 2001). In our study we employed a multi-instrument approach, using active and passive remote sensors, either ground- or space-based, namely a LIDAR system, a sun photometer and satellite data.

The LIDAR technique is based on the emission of a collimated laser beam in the atmosphere and on the detection of the backscattered laser light by the suspended atmospheric aerosols and atmospheric molecules. The LIDAR technique, through its high temporal (from seconds to minutes) and spatial (3–15 m) resolution, is a powerful tool to visualize in real time, the structure of the PBL using the aerosols as passive tracers of the atmospheric dynamic processes. A backscattering LIDAR can thus provide information on the PBL's mixed layer depth, entrainment zones and convective cells structure, aerosol distribution, clear air layering, cloud-top altitudes, cloud statistics, atmospheric transport processes and other inferences of air motion (Ferrare et al., 1991; Melfi et al., 1985; Crum et al., 1987; Balis et al., 2000; Papayannis and Chourdakis, 2002).

The sun photometer data are used to provide AOT values at selected wavelengths and thus to derive the Angstroem Exponent values over S. Paulo. The synergy of CIMEL and LIDAR measurements also acts in minimizing the uncertainties of the assumptions made, especially when inverting the LIDAR signal, using the Klett's technique (Klett, 1985). Aerosol optical thickness measurements performed with the sunphotometer were taken under 'cloud free' conditions during the last period of the wintertime, September and October months in 2001, and in August and September 2002. The first set of CIMEL data are level 2, denominated as quality assured data (Holben et al., 1998; Smirnov et al., 2000), while those of 2002 are only cloud screened data, since the calibration procedure had not been applied yet, when this paper was

ACPD
3, 2835–2877, 2003

prepared.

Some selected days were taken as case studies and for these days air mass backward trajectories were calculated using the University of São Paulo Back Trajectory Model (USPTM) (Freitas et al., 1996) in order to determine the height and origin of the aerosol load entering MASP. For the purpose of identifying the origin of remote sources of aerosols we took the images from the Moderate Resolution Imaging Spectroradiometer (MODIS) aboard of the Terra Satellite.

2. The experimental set-up

The LIDAR system operated over the city of São Paulo is a coaxial mode single-wavelength backscatter system pointing vertically to the zenith. The light source is a commercial pulsed Nd:YAG laser operating at the second harmonic frequency (532 nm) with a fixed repetition rate of 20 Hz. The average power can be selected as high as 3.3 W and the emitted laser beam has 7 mm diameter and a divergence of 0.5 mrad. The laser beam is sent to the atmosphere through a Newtonian telescope, which is equipped with a 30 cm receiving mirror and has a 1.3 m focal length. The optics set-up is such that the maximum overlap is reached at about 350 m above the LIDAR system (Chourdakis et al., 2002). The backscattered laser radiation is detected by a S-20 photo-multiplier tube (PMT) and a narrow band (1 nm FWHM) interference filter at 532 nm is used to select the desired wavelength and assure the efficient reduction of the background skylight during daytime operation, thus, improving the signal-to-noise ratio at 532 nm. The PMT output signal is recorded in the analog mode by a 1-GSa/s digitising oscilloscope (DSO), having 11-bit resolution of analog-to-digital conversion (ADC). Data are averaged every 2 to 5 min, with a typical spatial resolution of 15 to 30 m.

As stated before, co-located CIMEL aerosol measurements were performed to determine the AOT values at several wavelengths in the visible spectrum and thus to enable the assessment of the AE values at the same spectral region. The principle

ACPD
3, 2835–2877, 2003

of operation of the CIMEL instrument is to acquire aureole and sky radiances measurements. The standard measurements are taken 15 min apart, in order to allow for cloud contamination checking. These measurements are taken in the whole spectral interval, and their number depends on the daytime duration. The instrument precision and accuracy follow the standard Langley plot method within the standard employed by the AERONET network (Holben et al., 1998). The CIMEL sun photometer is calibrated periodically by a remote computer or locally under the supervision of the AERONET network. The calibration methodology assures a coefficient accuracy between 1 and 3%, nonetheless various instrumental, calibration, atmospheric, and methodological factors influence the precision and accuracy of optical thickness and effectively the total uncertainty in the AOT retrieved values is less than 8% (Balis et al., 2000).

3. Methodology and data analysis

3.1. LIDAR data retrieval

In the present stage, the retrieval of the aerosol optical properties is based on the measurements of the aerosol backscattering coefficient (β_{aer}) at 532 nm, up to an altitude of 5–6 km. The determination of the vertical profile of the aerosol backscatter coefficient relies on the LIDAR inversion technique following the Klett's algorithm, as proposed by Klett (1985). One has however to bear in mind that this inversion technique is an ill-posed problem in the mathematical sense, leading to errors as large as 30% when applied (Papayannis and Chourdakis, 2002). In general, the inversion of the LIDAR profile is based on the solution of the LIDAR equation, under the assumption of the single scattering approximation:

$$P(\lambda, R) = P_L \left(\frac{c\tau}{2}\right) \beta(\lambda, R) A_0 \xi(\lambda) \xi R^{-2} \exp\left[-2\int_0^R \alpha(\lambda, r) dr\right], \quad (1)$$

ACPD
3, 2835–2877, 2003

where $P(\lambda, R)$ is the LIDAR signal received from a distance R at the wavelength, P_L is the emitted laser power, A_0 is the telescope receiving area, $\xi(\lambda)$ is the receiver's spectral transmission factor, $\beta(\lambda, R)$ is the atmospheric volume backscattering coefficient, $\xi(R)$ is the overlap factor between the field of view of the telescope and the laser beam, $\alpha(\lambda, R)$ is the extinction coefficient, c is the light speed and t is the laser pulse length.

In this equation, the coefficients β and α can be separated in two sets, one for the molecular scattering component and the other for the particle scattering component. Besides, in the Klett's inversion technique, there is a reference altitude, Z_{ref}, which is used as an upper limit, and has to be an aerosol-free region. Therefore, in this region and above it, the LIDAR signal shows a decay, which follows the molecular contribution only. This is regularly checked using the technique proposed by Chourdakis et al. (2002), which assures the perfect alignment of the LIDAR system.

As stated before, to retrieve the aerosol backscatter coefficient we applied the Klett's inversion technique assuming a "guessed" altitude-constant extinction-to-backscatter ratio (LR) in the lower troposphere. It is known that the LR depends on several parameters, such as the aerosol refractive index, the shape and size distribution of the aerosol particles. Besides, there is a strong dependence of LR on the temperature and humidity profiles in the atmosphere, that might cause variations on the optical parameters of the aerosols (Haenel, 1976), and of course on the presence of turbulence in the atmospheric volume being probed by the LIDAR beam (Stull, 1991).

To derive the appropriate "correct" values of the vertical profile of aerosol backscatter coefficient in the lower troposphere we used an iterative inversion approach (by "tuning" the LR values) based on the inter-comparison of the AOT values derived by LIDAR and CIMEL data, assuming the absence of stratospheric aerosols and that the PBL is homogeneously mixed between ground and 300 m height, where the lidar overlap factor is close to 1. Once the "correct" values of the vertical profile of aerosol backscatter coefficient were derived (when the difference of the AOTs derived by CIMEL and LIDAR was less than 10%) we reapplied the Klett method, using the appropriate LR values, to retrieve the final values of the vertical profiles of the backscatter and extinction

ACPD
3, 2835–2877, 2003

coefficient at 532 nm.

3.2. Sunphotometer data retrieval

The inversion of the solar radiances measured by the CIMEL sunphotometer to retrieve the aerosol optical thickness values, is based on the Beer-Lambert Eq. (2), assuming that the contribution of multiple scattering within the small field of view of the sunphotometer is negligible:

$$I_\lambda = I_\lambda^0 \exp(-\tau_\lambda/\mu_s), \tag{2}$$

where I_λ and I_λ^0 are the solar irradiances at the top of the atmosphere and at ground level, respectively, and μ_S is the cosine of the solar zenith angle. τ_λ is the total atmospheric optical thickness from the Rayleigh and aerosol contributions, as well the ozone and water vapour absorption at 670 nm and 870 nm, respectively. The molecular (Rayleigh) scattering contribution is taken into account to retrieve the aerosol optical thickness values at 532 nm, determined by the relation:

$$\frac{\tau_{532}^{\text{aer}}}{\tau_{500}^{\text{aer}}} = \left(\frac{532}{500}\right)^{\mathring{a}}, \tag{3}$$

where the Ångström exponent (Ångström, 1964) $\mathring{a}$ was derived from the measured optical thickness in the blue and red channels (440 nm and 670 nm):

$$\mathring{a} = -\frac{\log\left(\tau_{440}^{\text{aer}}/\tau_{670}^{\text{aer}}\right)}{\log(440/670)}. \tag{4}$$

3.3. 3D back-trajectory model

The air-mass backward trajectory calculations apply a 3-dimensional (3D) kinematic trajectory model which was developed at the University of São Paulo (Freitas et al., 1996; Freitas et al., 2000). The air mass trajectories (called kinematic trajectories) are

ACPD
3, 2835–2877, 2003

obtained using the three components of the wind field, which is numerically generated by the Regional Atmospheric Modelling System approach (RAMS) as shown by Pielke et al. (1992) and by Liston and Pielke (2001). The air parcel trajectory output is generated every 3 min, thus providing the latitude, longitude and altitude coordinates. In this paper we show the trajectory locations every 6 h using a colour-coded scale. The model time period extends to about one week, while the corresponding spatial resolution is about 60 km (Freitas et al., 2000). In this paper we calculated 96-hours (4 days) back-trajectories of air masses ending over the city of São Paulo, in order to have a more realistic input about the origin of the air masses ending over our LIDAR site and to locate the aerosols sources near the São Paulo region.

3.4. The MODIS sensor

The Moderate Resolution Imaging Spectroradiometer (MODIS) was launched in December 1999 on the polar orbiting Terra spacecraft and since February 2000 has been acquiring daily global data in 36 spectral bands from the visible to the thermal infrared (29 spectral bands with 1 km, 5 spectral bands with 500 m, and 2 with 250 m nadir pixel dimensions). The Terra satellite has on-board exterior orientation (position and attitude) measurement systems designed to enable the geolocation of MODIS data to approximately 150 m at nadir. A global network of ground control points is being used to determine biases and trends in the sensor orientation. Biases have been removed by updating models of the spacecraft and instrument orientation in the MODIS geolocation software several times since launch and have thus improved the MODIS geolocation to approximately 50 m at nadir. The Terra and Aqua spacecrafts orbit the Earth at an altitude of 705 km in a near polar orbit with an inclination of 98.2° and a mean period of 98.9 min (Salomonson et al., 1989).

Terra's sun-synchronous orbit has a dayside equatorial 10:30 a.m. local crossing time and a 16-day repeat cycle. MODIS has a 110° across-track field of view and senses the entire equator every 2 days with full daily global coverage above approximately 30° latitude (Wolf et al., 2002). MODIS is a paddle broom (sometimes called

ACPD
3, 2835–2877, 2003

a whiskbroom) electro-optical instrument that uses the forward motion of the satellite to provide the along-track direction of scan. The electromagnetic radiation (EMR) reflected or emitted from the Earth is reflected into the instrument telescope by a rotating two-sided scan mirror. One-half revolution of the scan mirror takes approximately 1.477 s and produces the across-track scanning motion. The EMR is then focused onto separate calibrated radiation detectors covered by narrow spectral band-pass filters. MODIS simultaneously senses, in each band, 10 rows of 1 km detector pixels, 20 rows of 500 m detector pixels, and 40 rows of 250 m detector pixels. Each row corresponds to a single scan line of MODIS data that is nominally composed of 1354 (1 km detector pixels), 2708 (500 m detector pixels) and 5416 (250 m detector pixels) observations.

4. Experimental data – dry season year 2001 and 2002

The first LIDAR measurements started over São Paulo in August 2001. For the so-called dry season we selected some specific cloud-free days in the years 2001 and 2002, where CIMEL, lidar and satellite date were available and were typical for the aerosol loadings over the city of São Paulo. Table 1 summarizes the dates of simultaneous CIMEL and LIDAR measurements during the dry season months of the years 2001 and 2002.

As previously mentioned the meteorological conditions during the dry season are favourable to air pollution increase over the city and usually are accompanied by the formation of a thermal inversion typically 1000–1200 m above ground level. Therefore, the majority of the aerosol load is trapped inside the PBL, which means between ground level and the top of the mixing layer (ML), typically 1 km above the ground. Figures 1 to 5 show some typical aerosol backscatter profiles obtained at 532 nm during selected days of the dry season period (Table 1). These profiles are sorted in three categories according to some common features of the vertical distribution of the aerosol backscatter coefficient:

ACPD
3, 2835–2877, 2003

4.1. Category A

The mean aerosol backscatter profiles obtained on 19 September 2001 (Fig. 1) and on 20 August 2002 (Fig. 2) show that the majority of the aerosol load is confined between ground level and 1000–1250 m height. These days the mixing layer did not evolve to higher heights and thus an almost aerosol free atmosphere is found above 1500–2000 m height. In this context the aerosol load observed inside the PBL sources is due mainly to local urban activities, like car traffic, industrial emissions and other urban sources.

The AOT values obtained at 532 nm on 19 September 2001, were 0.12 ± 0.02 and 0.13 ± 0.03 for the CIMEL and LIDAR systems, respectively, taking into account that the LR input value, for the Klett's inversion, was taken equal to 45 sr. Similar values of the LR at 532 nm were reported by Mueller et al. (2001) and by Wandinger et al. (2002) for urban air polluted air masses during the INDOEX experiment. The 10% difference found between the AOT derived by the CIMEL and LIDAR data could be attributed to the first 300 m not probed by the LIDAR system. As mentioned previously, in these first 300 m of the atmosphere, the overlap factor is less than 1 (Measures, 1989). If we assume a well-mixed PBL up to 300 m height, the corresponding AOT derived by the LIDAR data inversion becomes then equal to 0.15. If we want to "match" the AOT value derived by LIDAR to that of CIMEL (AOT=0.12), including the first 300 m, we should then consider a LR input value equal to 36 sr.

In the case of day 20 August 2002, the AOT values derived by CIMEL and LIDAR data were 0.10 and 0.05, respectively. In this case the lidar data underestimated the AOT at 532 nm. If we include again the first 300 m assuming again well-mixed atmospheric conditions inside this layer, we then find an AOT of the order of 0.09 (LIDAR data) assuming a LR input value of 48 sr. The difference between CIMEL and LIDAR data values stays within the 10% difference.

The Ångström exponent values calculated for these days are 1.9±0.3 (19 September 20010 and 1.5 ± 0.2 (20 August 2002). On 19 September 2001, since the value of *å*

ACPD
3, 2835–2877, 2003

is above 1.6, there is an indication of the presence of rather small aerosols of urban origin, like carbonaceous particles and of anthropogenic or biogenic sulphates. On 20 August 2002 the *å* value obtained indicates slightly larger particles present in the atmosphere, such as dust and mineral aerosols (Deepak and Gerber, 1983; D'Almeida et al., 1991).

4.2. Category B

The aerosol backscatter profile taken on 21 August 2002 between 12:00 and 13:00 GMT (Fig. 3) shows a different pattern, since one can observe various aerosol layers at about 750, 1500 and 4500 m height. Also at higher altitudes one can observe a discrete aerosol layer around 6000 m height. However, below 1000 m the absolute values of the aerosol backscatter coefficient are less important than those in category A. Concerning the potential aerosol sources one can still assume originating from the nearby regions mainly due to the urban activity concerning the first 1000 m. The discrete aerosol layers found higher than 2500 m can be attributed to the residual layer from the previous day or most probably to particles originating from more remote areas.

The average AOT value given that day by the CIMEL instrument for this time period was 0.13 ± 0.02, while the AOT derived from the LIDAR data was 0.12 ± 0.03 using an input value of LR equal to 45 sr. If we assume again well-mixed atmospheric conditions in the first 500 m of the troposphere, the AOT derived by the LIDAR profile becomes equal to 0.16. In order to 'match' the AOT value derived by the LIDAR to that of CIMEL within the 10% criterion and to include the first 500 m of the atmosphere, we should assume a LR input value of 37 sr. This is again well comparable with the LR values found during the INDOEX experiment in the Asian tropical regions over urban areas (Mueller et al., 2001; Wandinger et al., 2002). The Ångström exponent value of 1.1 ± 0.2 found that day points out to the presence of bigger particles in the atmosphere (than in category A), such as mineral aerosols and sulphates, indicating as their possible origin the industrial and urban activities in the city.

ACPD
3, 2835–2877, 2003

4.3. Category C

The aerosol backscatter profiles taken between 13:00 and 14:00 GMT, on 24 September 2001 and 23 August 2002 are shown in Figs. 4 and 5. In both profiles intense aerosol layers are present around 1500–2000 m and above 2500 m. These aerosol layers as well as the very thick layer observed between 2500 and 6000 m, are indicative of the presence of long-range transported particles in the free troposphere originating from remote areas. The mean AOT derived values from the CIMEL data at 532 nm on 24 September 2001, were quite high, of the order of 0.35. If we include again the assumed well-mixed first 300 m and match the LIDAR and CIMEL AOT values to within 10%, we find a mean LR of the order of 41 sr. The Ångström exponent value obtained for this day was found to be 1.6 ± 0.2 indicating the presence of rather small aerosol particles, such carbonaceous particles or even smoke aged aerosols diluted over the urban area of São Paulo (Eck et al., 1999).

The value of the AOT for 23 August 2002 derived by the CIMEL instrument was again quite high (0.30). If again we match the AOT values derived by the CIMEL and LIDAR systems to within 10% and make similar assumptions of well-mixed air masses in the first 300 m, we find a mean LR at 532 nm of 65 sr. This value is indicative of highly absorbing aerosol particles. This value is typical for biomass burning aerosols in the tropics, as shown by Mueller et al. (2001) during the INDOEX campaign and by Balis et al. (2003) during a large biomass burning event recently observed over Europe. The intense aerosol layers observed in Category C files at altitudes higher than 2.5 km could be therefore attributed to long-range transported biomass burning aerosols. This could be verified by analysing the corresponding satellite data and by using air mass back-trajectory analysis.

ACPD
3, 2835–2877, 2003

5. Satellite data and air mass back trajectory analysis

To identify the source of high aerosol loadings observed over Sao Paulo region during the dry season we performed air mass back trajectory analysis with conjunction with satellite data derived from the MODIS sensor. We did not use the TOMS aerosol index data since TOMS is unable to reveal aerosol layers below 2.5 km height (Herman et al., 1996). The MODIS AOT data over the São Paulo region are shown in Figs. 6 to 12 for 19, 20 and 24 September 2001 and for 19, 20, 21 and 23 August 2002, respectively.

For the days of category A (19 September 2001 and 20 August 2002) the AOT data obtained by MODIS (Figs. 6 and 10, respectively) show low (0.1) AOT values over São Paulo and higher AOT values (0.35–0.5) west of the city, indicating the existence of regions where biomass burning activities are taking place during the dry season. On the day of category B (21 August 2002) the MODIS AOT data (Fig. 11) over São Paulo indicated AOT values similar to those retrieved by the CIMEL, which were of the order of 0.10–0.15, while again higher AOT values were found south-east of the city indicating the presence of advected aerosol particles (0.2<AOT<0.35) probably from the biomass burning or industrial regions inland. The MODIS AOT data for the days of category C (24 September 2001 and 23 August 2002) indicated AOT values over the city, of the order of 0.2–0.25 (Fig. 8) and of 0.15–0.20 (Fig. 12), respectively. One can also observe important AOT values (0.30–0.50) west of the city of São Paulo, which could be due to biomass burning aerosols. Important AOT values (0.15–0.30) were also observed south of the city on 23 August 2002, which again could be advected biomass burning aerosols.

We will focus now on the air mass trajectories ending at various heights over our LIDAR and CIMEL site only during the days of category C, where the largest AOT values were measured. Figures 13 to 15 show the 96-hours air mass back trajectories ending at 12:00 GMT on 24 September 2001 at 1000 m, 2000 m and 4500 m above the LIDAR site, respectively. The air mass back trajectory plots are shown in an altitude-to-colour scale, and every interval between the white dots in the trajectories corresponds

ACPD
3, 2835–2877, 2003

to a time step of 6 h. As shown in Fig. 13 the air masses ending at 1000 m height originated from the Atlantic Ocean around 2 km height, thus maritime aerosols should be predominant. On the other hand, the air masses ending at 2000 m height (Fig. 14), where an important aerosol layer was observed (Fig. 4), came from the north-western direction and originated 4 days earlier at 1000 m height (on 20 September 2001) from a region where biomass burning is very common during the dry season. This indeed is verified by the MODIS data of that day (Fig. 7) where high AOT values (0.35–0.5) were observed north-west of the city of São Paulo. The air masses ending at 4500 m (Fig. 15) had a completely different origin. They originated 4 days before from a south-western direction, at the same altitude region, bringing probably continental biomass burning aerosols, which are observed as a 2 km thick aerosol layer between 3.5 and 5.5 km height. It is interesting to note that on 24 September 2001 the air masses ending over São Paulo at various heights up to 4500 m had completely different origins, thus carrying different types and sizes of aerosol particles (maritime, continental, urban and biomass burning aerosols).

On 23 August 2002 the 96-hours air mass back trajectories ending at 1000 m, 1900 m, 4000 m and 5400 m over São Paulo are shown in Figs. 16 to 19, respectively. At 1000 m and 1900 m end points we get air parcels from the north originating from the Atlantic Ocean, around 1900–2000 m height, and carrying mostly maritime aerosols. The MODIS AOT data for the previous days all indicated the advection of important aerosol loadings south of the city of São Paulo, as shown in Figs. 9 to 11. This load could be related advected biomass burning aerosols coming form the north-western part of the city, as shown by the back trajectory analysis for air masses ending at altitude levels between 4000 m and 5400 m. (Figs. 18 and 19) and the corresponding MODIS AOT data on 19 August 2002 (Fig. 9).

ACPD
3, 2835–2877, 2003

6. Discussion and concluding remarks

In this paper we presented synergetic measurements of aerosols over the São Paulo area, using lidar, sunphotometer and satellite data. The aerosol backscatter profiles at 532 nm were obtained during the dry season of the years 2001 and 2002. Out of 51 vertical profiles of the aerosol backscatter coefficient we presented 5 selected profiles, which were sorted in three categories according to some common features of the vertical distribution of the aerosol backscatter coefficient.

The Klett inversion technique was applied in an iterative mode, with the synergy of the CIMEL data. Using this synergetic approach we derived a matched lidar ratio (LR) at 532 nm during each case of aerosol lidar profiles during the dry season. The mean value of LR found during the dry season was 45 sr, which is quite similar to the one found over urban areas during the INDOEX campaign by Mueller et al. (2001) and by Wandinger et al. (2002). One has of course to comment that the CIMEL data provides only the LR at 440 nm and so the wavelength dependence here could be a critical parameter we might be overlooking. However, Mie-scattering computations done by Deirmendjian (1969) show that the atmospheric volume backscattering coefficient does not change substantially in the 400–600 nm region.

Anyway, this issue should be indeed inspected in more details. Of course, a much larger number of aerosol backscatter profiles has to be collected over the São Paulo area, ideally with combination with a two-wavelength Raman lidar system (at 355 and 532 nm) and the CIMEL sun photometer so that a typical value of the LR could be derived during the dry season. Taking now into account all lidar measurements acquired during the dry season we made a category frequency histogram shown in Fig. 20. From this histogram one realizes that majority of days, namely 23, are categorized as B, that means there are some layers mixed up to 3 km, however their absolute value is close to an aerosol free atmosphere, this category represents 45% of all days.

The second most frequent category is the A category, which is related to a low layer, up to 2 km, and a very “clean” atmosphere higher up, this category is about

ACPD
3, 2835–2877, 2003

31% of all days, we have also seen that the A category examples we took are those with the lowest values of AOT, these days, in general follow a meteorological condition which favoured the dispersion of pollutants, either by rainy days, which washed out the atmosphere, or those preceding a cold front, which are in general windy days. Finally, there are the days related to the C category, which represent 24% of all days we took measurements, those days are, from the point of view of the origin of the air masses the most interesting since the air parcels probed over São Paulo were rich in long-range transported aerosols structured in distinct layers in the free troposphere and also they presented the highest AOT values.

As a summary important aerosol loads were observed over the city of São Paulo, Brazil during the dry season, using a single-wavelength LIDAR system operating at 532 nm and a CIMEL automatic sun photometer. The LIDAR profiles revealed for the first time the existence of important quantities of aerosols at altitudes between 2500 and 5500 m above the LIDAR site, as well as in the altitude range between 1500 and 2000 m over the city of São Paulo. Three dimensional 96-hours air mass back-trajectory analysis showed that the aerosols detected at the higher altitudes may have originated from biomass burning activities taking place at the southern borders of the Amazon forest during the dry (fire) season.

The MODIS AOT data confirmed the existence of biomass burning regions over the Amazon forest. The LIDAR profiles also showed the presence of aerosols at altitudes around 1500–2000 m, which corresponded to the upper part of the Planetary Boundary Layer over the city of São Paulo or originated over the Atlantic Ocean. These air masses are strongly influenced by local urban air pollution sources and are loaded with important quantities of anthropogenic aerosol particles. Additional measurements of the aerosol optical thickness using a CIMEL sunphotometer, during the case studies analysed, showed increased values of AOT (0.2–0.5) mainly on 23 August 2002, related to long-range transported aerosols from biomass burning regions of the Amazon rain forest area.

It is evident from the present study that biogenic and anthropogenic aerosols are

ACPD
3, 2835–2877, 2003

responsible for the high aerosol loadings found in the upper part of the PBL and in the free troposphere over the city of São Paulo during the dry season. Considering the vast areas of tropical rain forests which are cleared every year by biomass burning activities in S. America and the high aerosol loads found in thus work during the dry season, biogenic and anthropogenic aerosol particles contribute in a major way to the AOT values observed and therefore these particles should play a very important role in the global aerosol budget. It is also evident that the lidar aerosol profiles obtained over São Paulo during the dry season could provide an important input for radiative transfer models (RTM) and atmospheric chemistry transport models (ACTM) over S. America.

Acknowledgements. The authors would like to thank for the financial support given by the Federal Agency Conselho Nacional de Desenvolvimento Cientifico e Tecnológico (CNPq) and by the State of São Paulo Agency Fundação de Amparo à Pesquisa (FAPESP) under contract numbers 620009/98-5 and 98/14891-2, respectively. The CIMEL data were provided by the AERONET network and the MODIS data were provided by ESA-NASA. The MODIS data used in this study were acquired as part of the NASA's Earth Science Enterprise. The algorithms were developed by the MODIS Science Teams. The data were processed by the MODIS Adaptive Processing System (MODAPS) and Goddard Distributed Active Archive Center (DAAC) and are archived and distributed by the Goddard DAAC.

References

Ackerman, J.: The extinction-to-backscatter ratio of tropospheric aerosol: A numerical study, J. Ocean. Atmos. Tech., 15, 1043–1050, 1998.

Alonso C. D. and Romano J.: São Paulo Metropolitan Area Air Quality Annual Report, São Paulo State Environmental Protection Agency – CETESB, 1999.

Angström, A.: The Parameters of Atmospheric Turbidity, Tellus, 16, 64–75, 1964.

Balis, D., Papayannis A., Galani, E., Marenco F., Santacesaria, V., Hamonou E., Chazette P., Ziomas, I., and Zerefos, C.: Tropospheric LIDAR aerosol measurements and sun photometric observations at Thessaloniki, Greece, Atmos. Environ., 34, 925–932, 2000.

Balis, D., Amiridis, V., Zerefos, C., Gerasopoulos, E., Andreae, M., Zanis, P., Kazantzidis, A., Kazadzis, S., and Papayannis, A.: Raman lidar and sunphotometric measurements of

aerosol optical properties over Thessaloniki, Greece during a biomass burning episode, Atmos. Environ., submitted, 2003.
Boesenberg, J.: EARLINET: A European Aerosol Research LIDAR Network, Adv. Laser Remote Sensing, Eds. A. Dabas, C. Loth and J. Pelon, 155–158, 2001.
Chourdakis, G., Papayannis A., and Porteneuve J.: Analysis of the receiver response for a non-coaxial LIDAR system with fiber-optic output, Appl. Opt., 41, 2715–2723, 2002.
Crum, T., Stull, R., and Eloranta, E.: Coincident lidar and aircraft observations of entrainment into thermal and mixed layers, J. Clim. Appl. Meteo., 26, 774–788, 1987.
D'Almeida, G. A., Koepke, P., and Shettle, E. P.: Atmospheric aerosols, Global climatology and radiative characteristics, Hampton, Virginia, 1991.
Deepak, A. and Gerber, H. E.: Aerosols and Their Climate Effects, Series Report 55, International Council of Scientific Unions and WMO, Switzerland, 1983.
Deirmendjian, D.: Electromagnetic scattering on spherical polydispersions, Elsevier Publ., New York, 1969.
Dubovik, O., Smirnov, A., Holben, B. N., King, M. D., Kaufman Y. J., Eck. T. F., and Slutsker, I.: Accuracy assessments of aerosol optical properties retrieved from Aerosol Robotic Network (AERONET) sun and sky radiance measurements, J. Geophys. Res., 105, 9791–9806, 2000.
Eck, T. F., Holben, B. N., Reid, J. S., Dubovik, O., Smirnov, A., O'Neill, N. T., Slutsker, I., and Kinne, S.: Wavelength dependence of the optical depth of biomass burning, urban, and desert dust aerosols, J. Geophys. Res., 104, 31 333–31 349, 1999.
Fernald, G. F.: Analysis of atmospheric LIDAR observations: some comments, Appl. Opt., 23, 652–653, 1984.
Ferrare , R., Schols, J., and Eloranta, E.: Lidar Observations of banded convection during BLX83, J. Appl. Meteor., 30, 312–326, 1991.
Freitas, S. R., Longo, K. M., Silva Dias, M. A. F., and Artaxo, P.: numerical modelling of air mass trajectories from the biomass burning areas of the Amazon Basin, Ann. Acad. Bras. de Sci., (In Portuguese), 68 (Supplement 1), 1996.
Freiras, S. R., Silva Dias, M. A. F., Dias, P. L. S., Longo, K. M., Artaxo, P., Andreae, M. O., and Fischer, H. S.: A convective kinematic trajectory calculation for low resolution atmospheric models, J. Geophys. Res., 105, 375–386, 2000.
Haenel, G.: The properties of atmospheric aerosol particles in function of the relative humidity at thermodynamic equilibrium with the scattering moist air, Adv. Geophys., 19, 73–188, 1976.
Hamonou, E., Chazette, P., Balis, D., Dulac, F., Schneider, X., Galani, E., Ancellet, G., and Pa-

payannis, A.: Characterization of the vertical structure of Saharan dust export to the Mediterranean Basin, J. Geophys. Res., 104, 22 257–22 270, 1999.
Herman, J. R., Bhartia, P. K., Krueger, A. J., Mcpeters, R. D., Wellemeyer, C. G., Seftor, C. J., Jaross, G., Schlesinger, B. M., Torres, O., Labow, G., Byerly, W., Taylor, S. L., Swissler, T., Cebula, R. P., and Gu, X.: METEOR-3 Total Ozone Mapping Spectrometer (TOMS) Data Products User's Guide, NASA Reference Publication, 1393, 1996.
Holben, B. N., Eck, T. F., Slutsker, I., Tanré, D., Buis, J. P., Setzer, A., Vermote, E., Reagan, J. A., Kaufman, Y. J., Nakajima, T., Lavenu, F., Jankowiak, I., and Smirnov, A.: Aeronet – A Federal instrument network and data archive for aerosol characterization, Rem. Sens. Environ., 66, 1–16, 1998.
Junge, C. E.: Air chemistry and radioactivity, Academic Press Inc, New York, New York, 1963.
Klett, J.: Lidar inversion with variable backscatter/extinction ratios, Appl. Opt., 24, 1638–1643, 1985.
Lelieveld, J., Crutzen, P. J., Ramanathan, V., et al.: The Indian Ocean Experiment: Widespread air pollution from South and Southeast Asia, Science, 291, 1031–1036, 2001.
Liston, G. E. and Pielke, R.: A climate version of the Regional Atmospheric Modelling System, Theor. Appl. Climatol., 68, 155–173, 2001.
Measures, R.: Laser Remote Sensing: Fundamentals and Applications, Krieger Publ. Company, Florida, 1992.
Melfi, S., Spinhirne, J., Chou, S-C., and Palm, S.: 1985, LIDAR observations of vertically organized convection in the planetary boundary Layer over the ocean, J. Clim. Appl. Meteor., 24, 806–821, 1985.
Mueller, D., Franke, K., Wagner, F., Althausen, D, Ansmann, A., Heintzenberg, J., and Verner, G.: Vertical profiling of optical and physical particle properties over the tropical Indian Ocean with six-wavelength lidar. 2 cases studies, J. Geophys. Res., 106, 28 577–28 595, 2001.
Pandis, S. N., Wexler A. S., and Seinfeld J. H.: Dynamics of tropospheric aerosols, J. Phys. Chem., 99, 9646–9659, 1995.
Papayannis, A. and Chourdakis, G.: The EOLE Project. A multiwavelength laser remote sensing (LIDAR) system for ozone and aerosol measurements in the troposphere and the lower stratosphere. Part II: aerosol measurements over Athens, Greece, Int. J. Rem. Sens., 23, 179–196, 2002.
Pielke, R. A., Cotton W. R., Walko, R. L., Tremback C. J., Lyons, W. A., Grasso, L. D., Nicholls, M. E., Moran, M. D., Wesley, D. A., Lee T. J., and Copeland, J. H.: A comprehensive meteo-

rological modelling system – RAMS, Meteo. Atmos. Phys., 49, 69–91, 1992.
Salomonson, V., Barnes, W., Maymon, P., Montgomery H., Ostrow, H.: MODIS – Advanced facility instrument for studies of the Earth as a system, IEEE Trans. Geos. Rem. Sens., 27, 145–153, 1989.
Saldiva, P. H. N., Pope, C. A., Scharwtz, J., Dockery, D. W., Lichtnfels, A. J., Salge, J. M., Barone, I., and Bohm, G. M.: Air pollution and mortality in elderly people: A time-series study in São Paulo, Brazil, Arch. Environ. Health, 50, 159–163, 1999.
Smirnov, A., Holben, B. N., Eck, T. F., Dubovik, O., and Slutsker, I.: Cloud-screening and quality control algorithms for the AERONET database, Remote. Sens. Environ., 73, 337–349, 2000.
Stull, R. B.: An Introduction to Boundary Layer Meteorology, 2nd edition (Boston, Kluwer Academic Publishers), 1991.
Wandinger, U., Mueller, D., Boeckmann, C., Althausen, D., Matthias, V., Boesenberg, J., Weib, B., Fiebig, M., Wendisch, M., Stohl., A., and Ansmann, A.: Optical and physical characterization of biomass burning and industrial pollution aerosols from multiwavelength lidar and aircraft measurements, J. Geophys. Res., 107, DOI 10.1029/2000, ID000202, 2002.
Wolf, E. R., Nishihama, A. M., Fleig, A. A., Kuyper, A. J., Roy, A. D., Storey, B. J., and Patt, G. F.: Achieving sub-pixel geolocation accuracy in support of MODIS land science, Rem. Sens. Environ., 83, 31–49, 2002.

Table 1. LIDAR and CIMEL measurements over São Paulo, during the dry season months of 2001 and 2002

Month and Year	Number of days with simultaneous CIMEL-LIDAR observations
August 2001	9
September 2001	8
October 2001	11
August 2002	15
September 2002	8

Table 2. List of selected days measured in the dry seasons of years 2001 and 2002 and the corresponding AOT, LR and Ångström Exponent values retrieved by sunphotometer (CIMEL) data

Day	Category	AOT CIMEL	LR CIMEL	Angst. Expon.
19/09/01	A	0.12±0.01	23	1.9±0.2
20/08/02	A	0.10±0.01	45	1.5±0.2
21/08/02	B	0.13±0.01	35	1.1±0.2
24/09/01	C	0.35±0.02	45	1.6±0.2
23/08/02	C	0.30±0.02	65	1.5±0.2

ACPD
3, 2835–2877, 2003

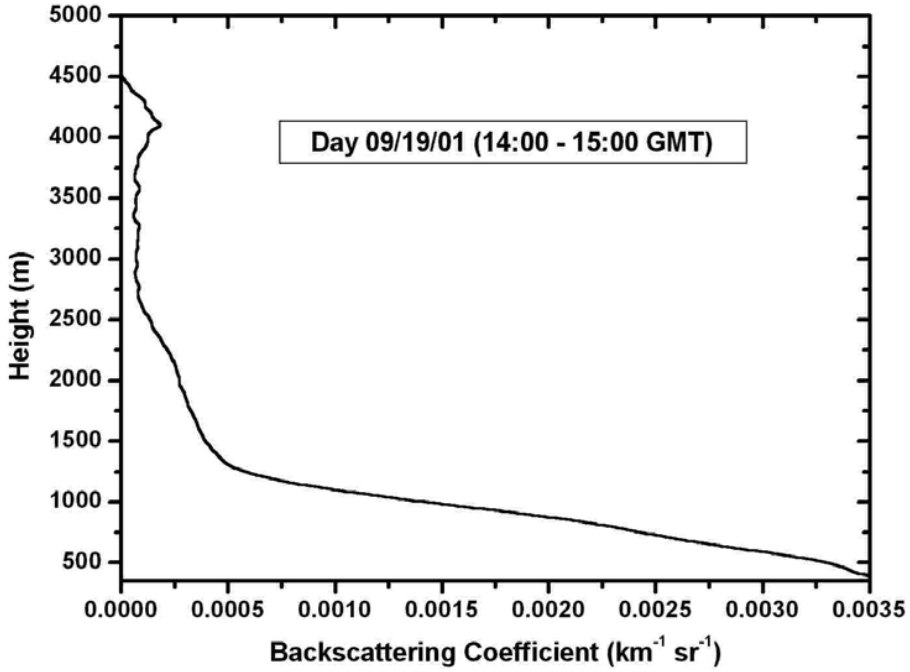

Fig. 1. Aerosol backscatter coefficient at 532 nm on 19 September 2001 (13:00–15:00 GMT).

ACPD
3, 2835–2877, 2003

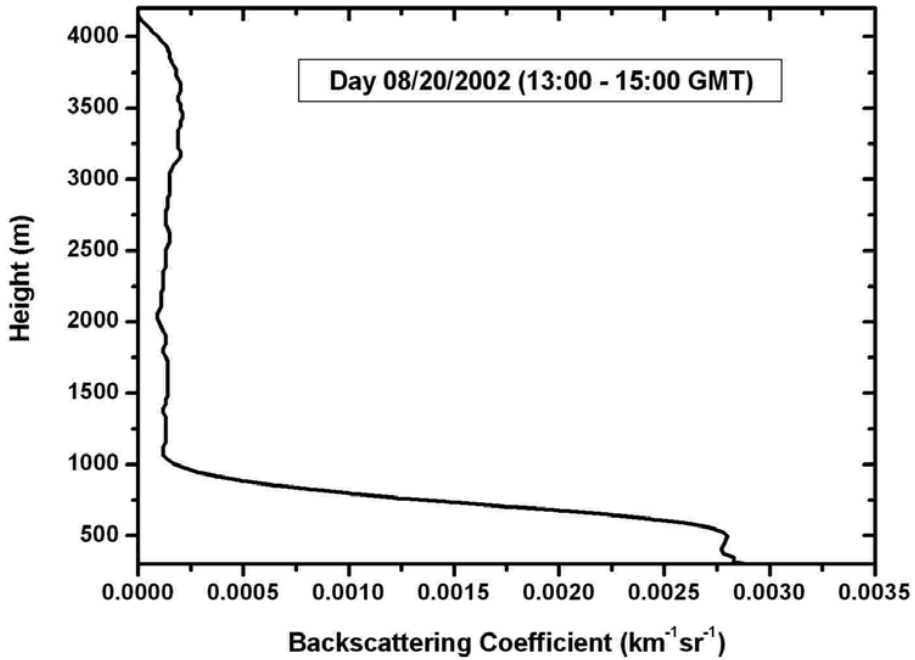

Fig. 2. Aerosol backscatter coefficient at 532 nm on 20 August 2002 (12:00–13:00 GMT).

ACPD
3, 2835–2877, 2003

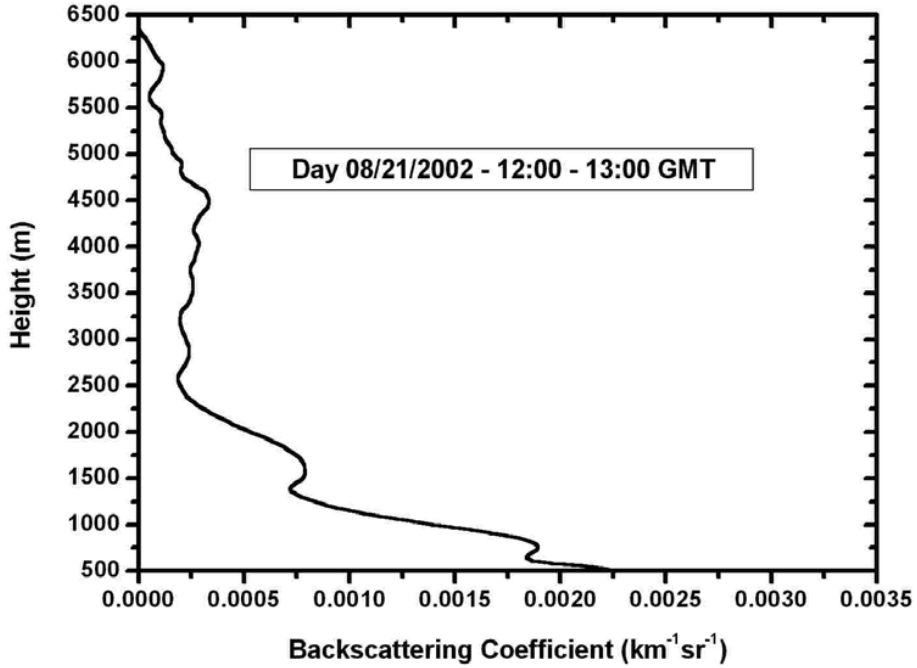

Fig. 3. Aerosol backscatter coefficient at 532 nm on 21 August 2002 (18:00–19:00 GMT).

ACPD
3, 2835–2877, 2003

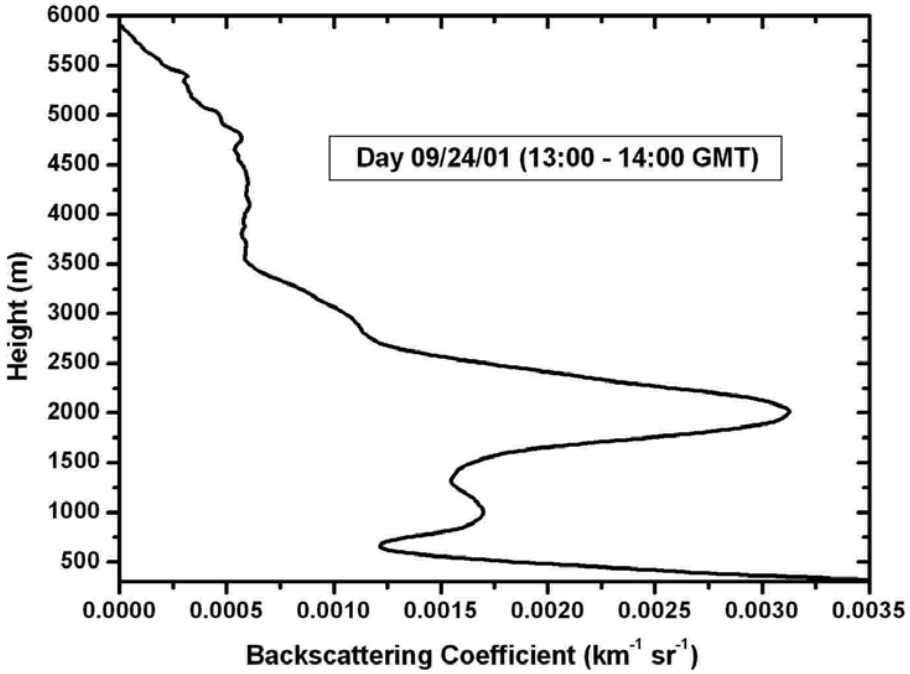

Fig. 4. Aerosol backscatter coefficient at 532 nm on 24 September 2001 (09:00–14:00 GMT).

ACPD
3, 2835–2877, 2003

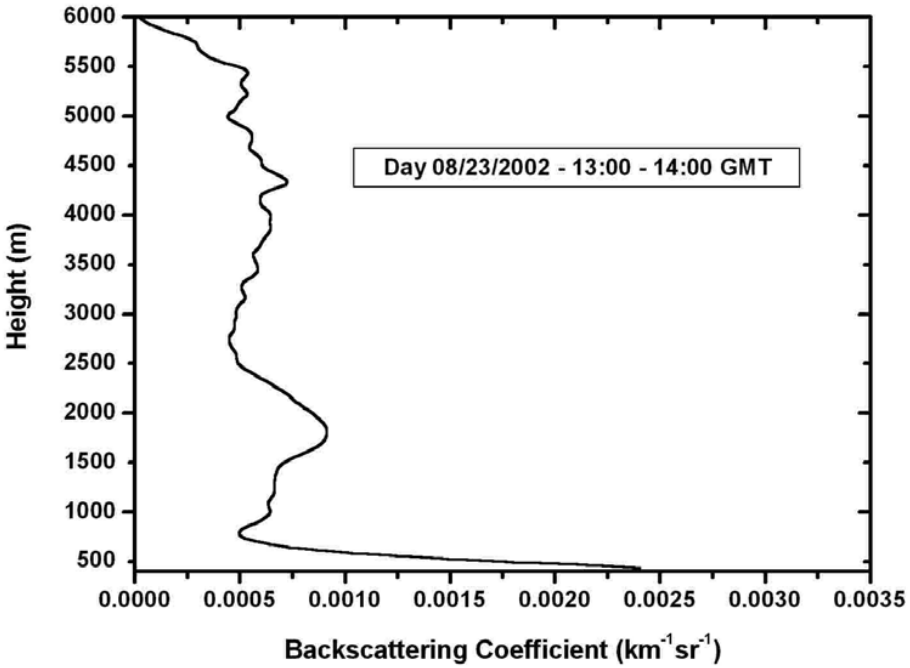

Fig. 5. Aerosol backscatter coefficient at 532 nm on 23 August 2002 (13:00–14:00 GMT).

ACPD
3, 2835–2877, 2003

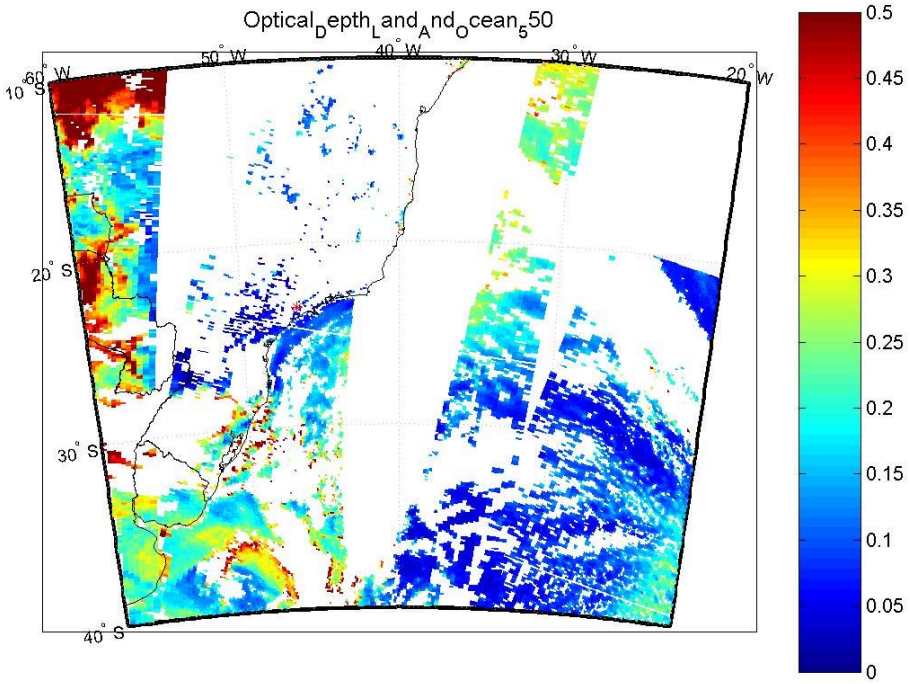

Fig. 6. MODIS AOT data on 19 September 2001 over São Paulo, Brazil.

ACPD
3, 2835–2877, 2003

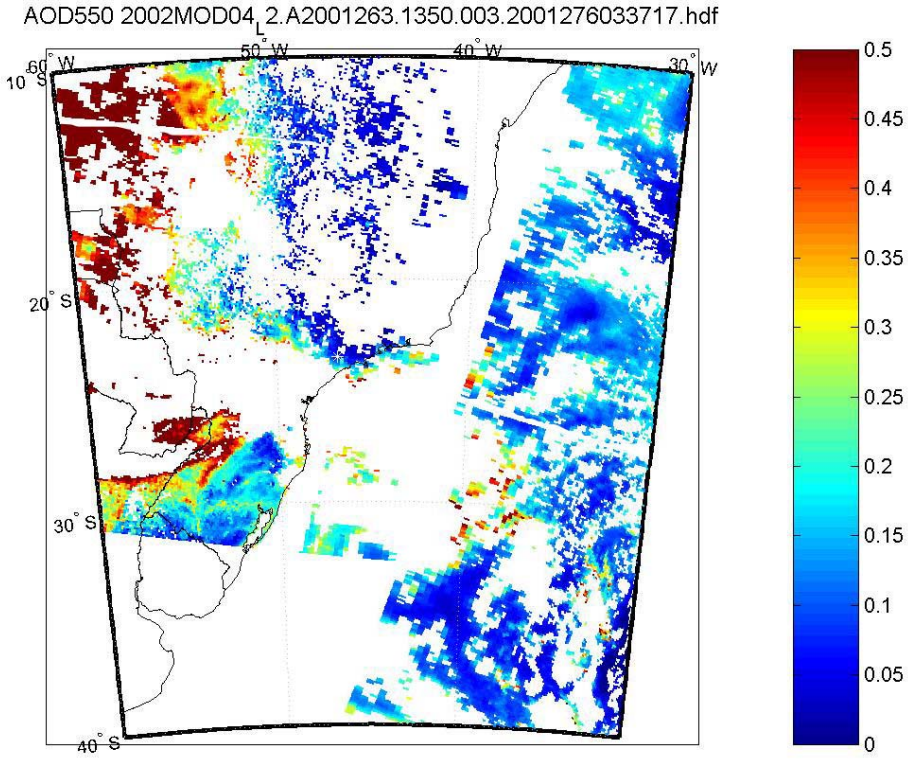

Fig. 7. MODIS AOT data on 20 September 2001 over São Paulo, Brazil.

ACPD
3, 2835–2877, 2003

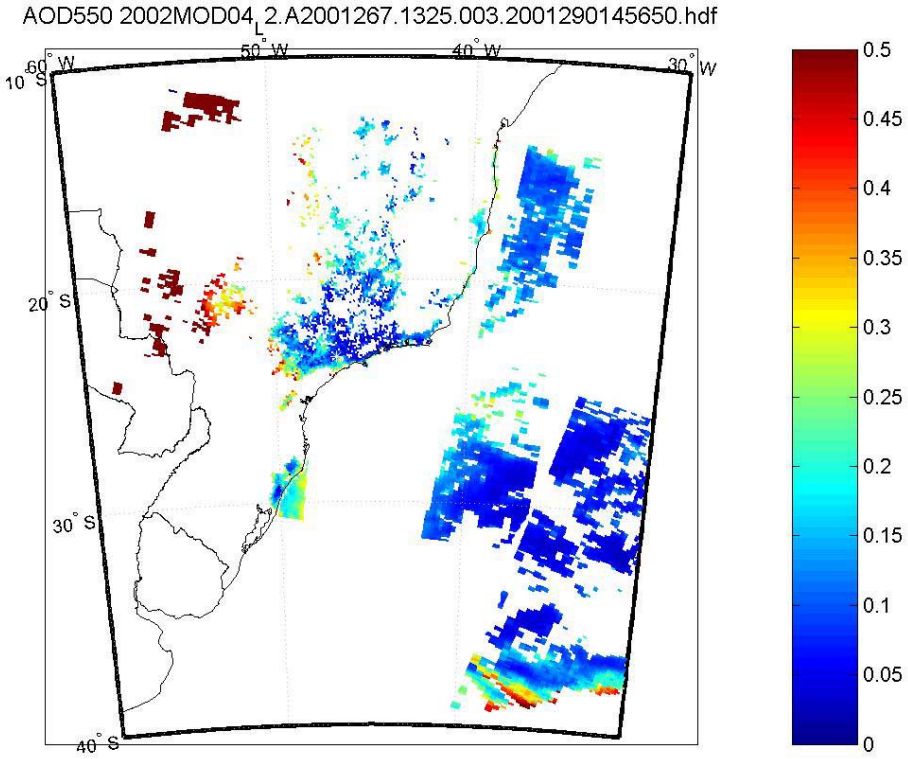

Fig. 8. MODIS AOT data on 24 September 2001 over São Paulo, Brazil.

ACPD
3, 2835–2877, 2003

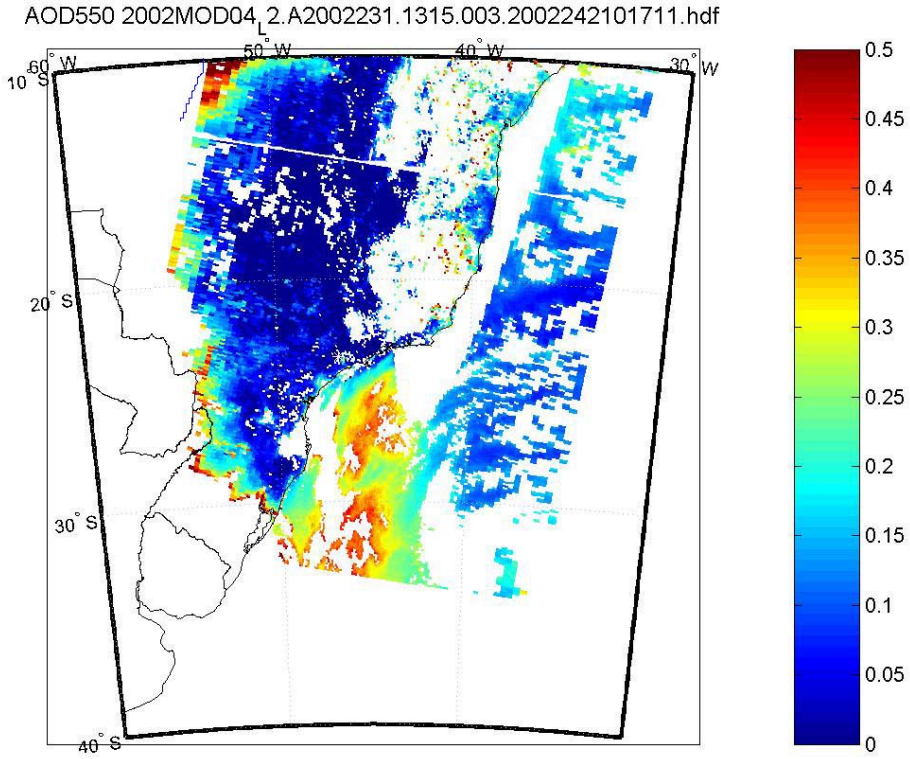

Fig. 9. MODIS AOT data on 19 August 2002 over São Paulo, Brazil.

ACPD
3, 2835–2877, 2003

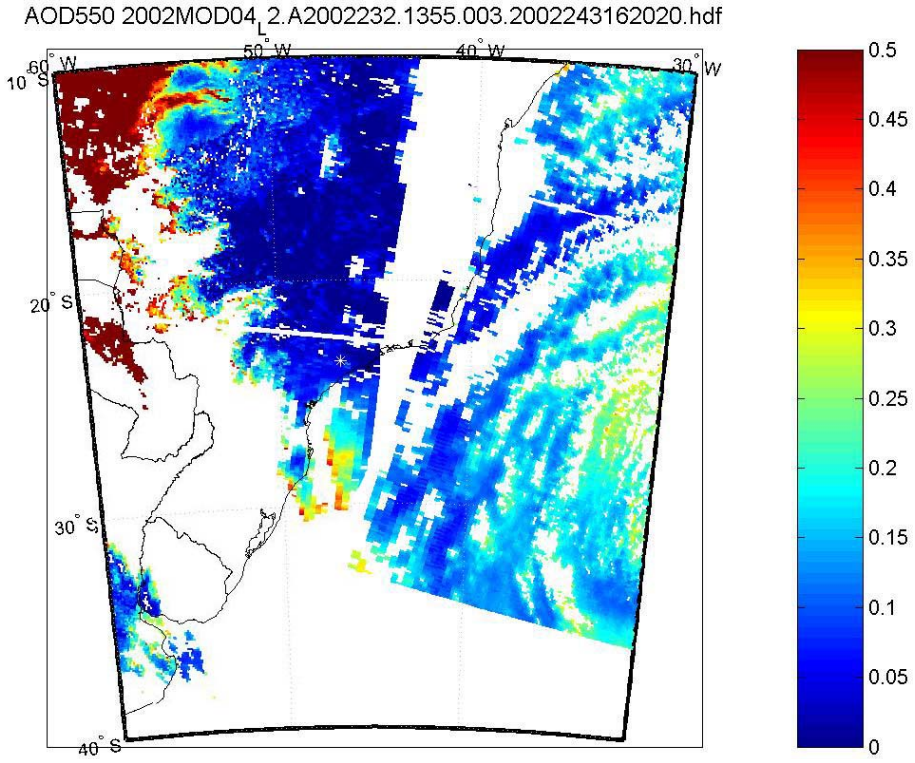

Fig. 10. MODIS AOT data on 20 August 2002 over São Paulo, Brazil.

ACPD
3, 2835–2877, 2003

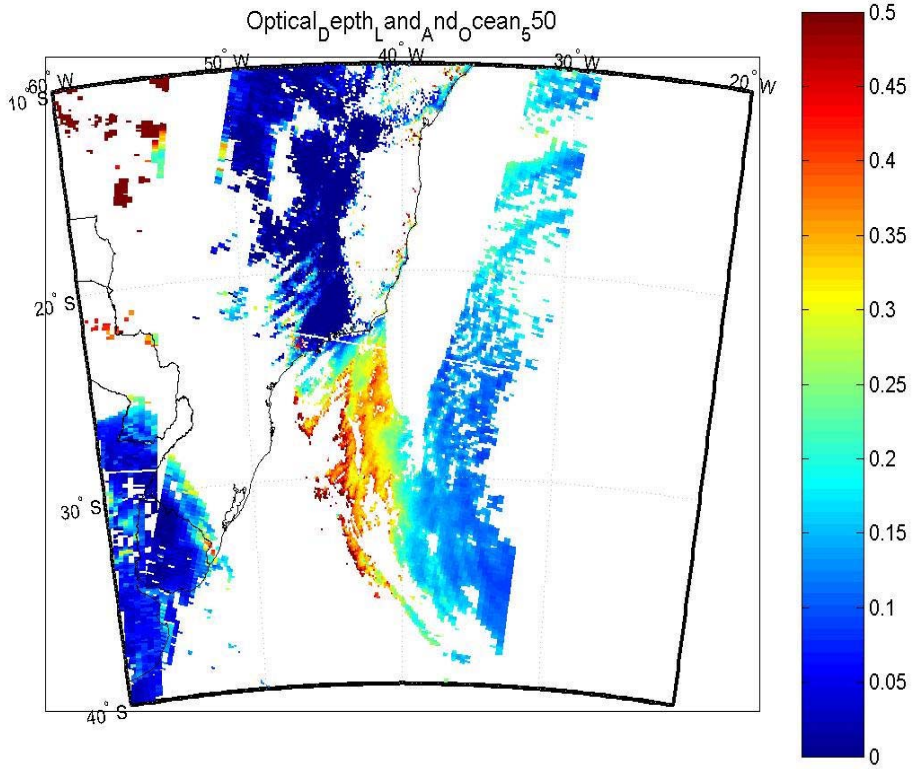

Fig. 11. AOT data on 21 August 2002 over São Paulo, Brazil.

ACPD
3, 2835–2877, 2003

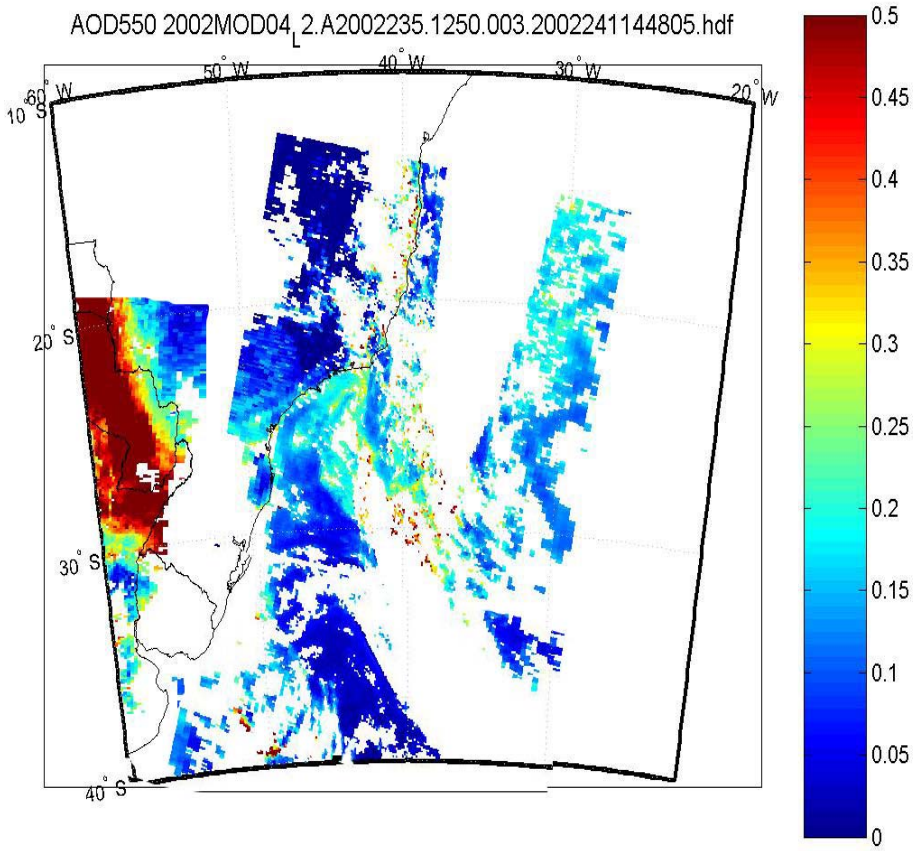

Fig. 12. MODIS AOT data on 23 August 2002 over São Paulo, Brazil.

ACPD
3, 2835–2877, 2003

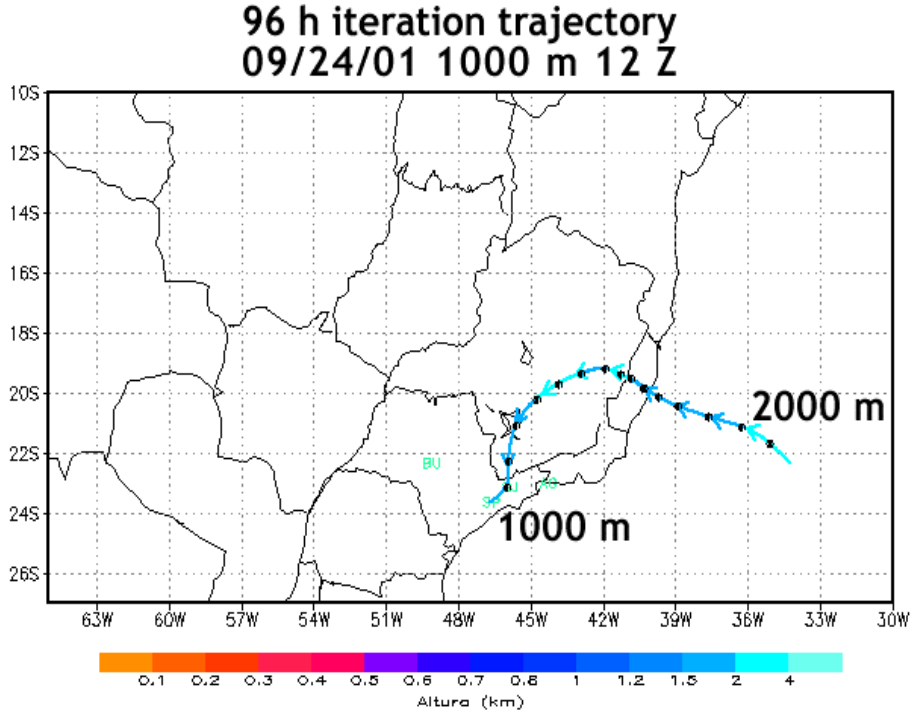

Fig. 13. 3D 96-hours air mass back-trajectory analysis for air masses ending over São Paulo, Brazil, on 24 September 2001 at 12:00 GMT at 1000 m.

ACPD
3, 2835–2877, 2003

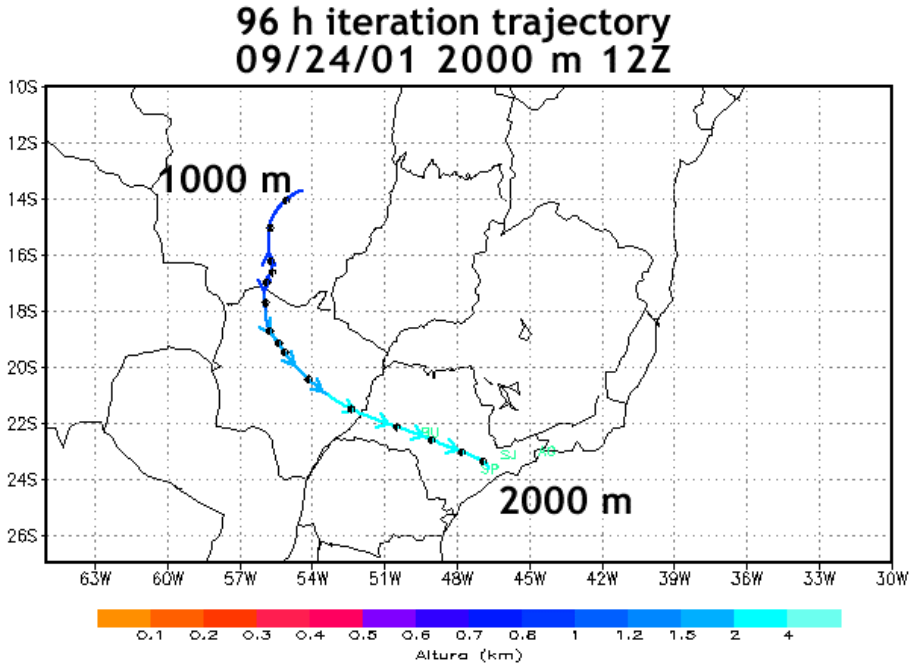

Fig. 14. 3D 96-hours air mass back-trajectory analysis for air masses ending over São Paulo, Brazil, on 24 September 2001 at 12:00 GMT at 2000 m.

ACPD
3, 2835–2877, 2003

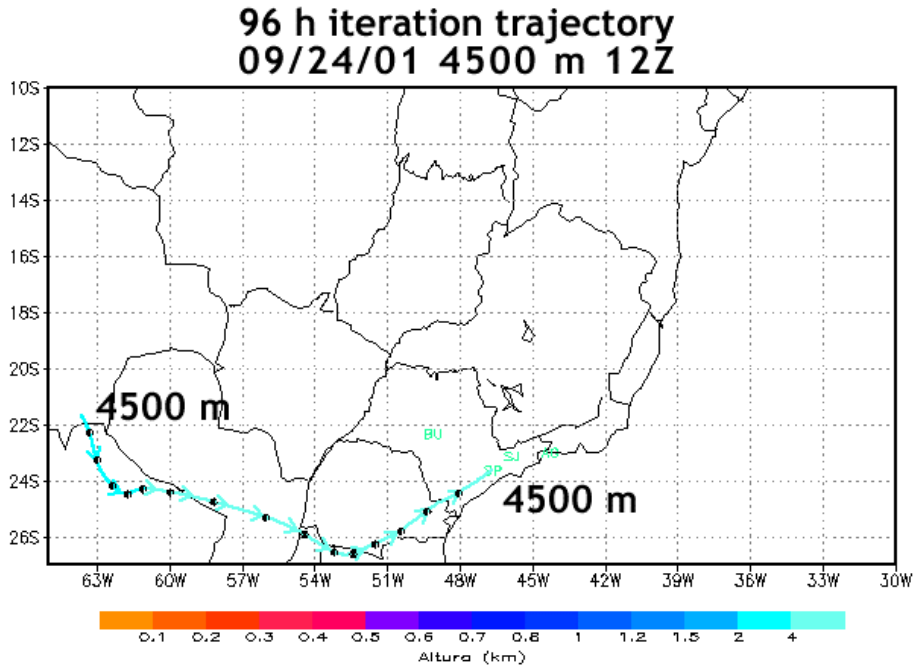

Fig. 15. 3D 96-hours air mass back-trajectory analysis for air masses ending over São Paulo, Brazil, on 24 September 2001 at 12:00 GMT at 4500 m.

ACPD
3, 2835–2877, 2003

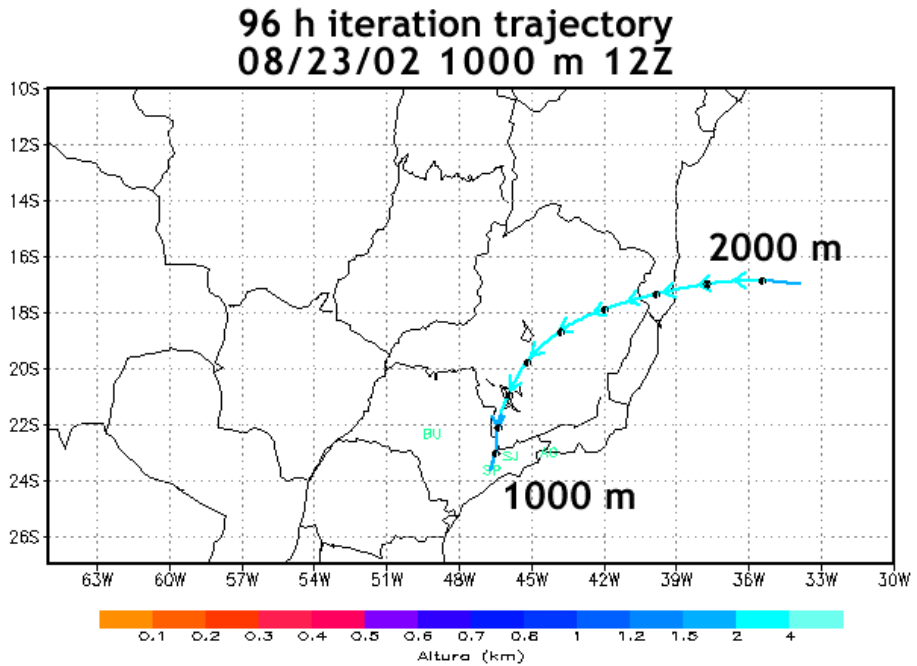

Fig. 16. 3D 96-hours air mass back-trajectory analysis for air masses ending over São Paulo, Brazil, on 23 August 2002 at 12:00 GMT at 1000 m.

ACPD
3, 2835–2877, 2003

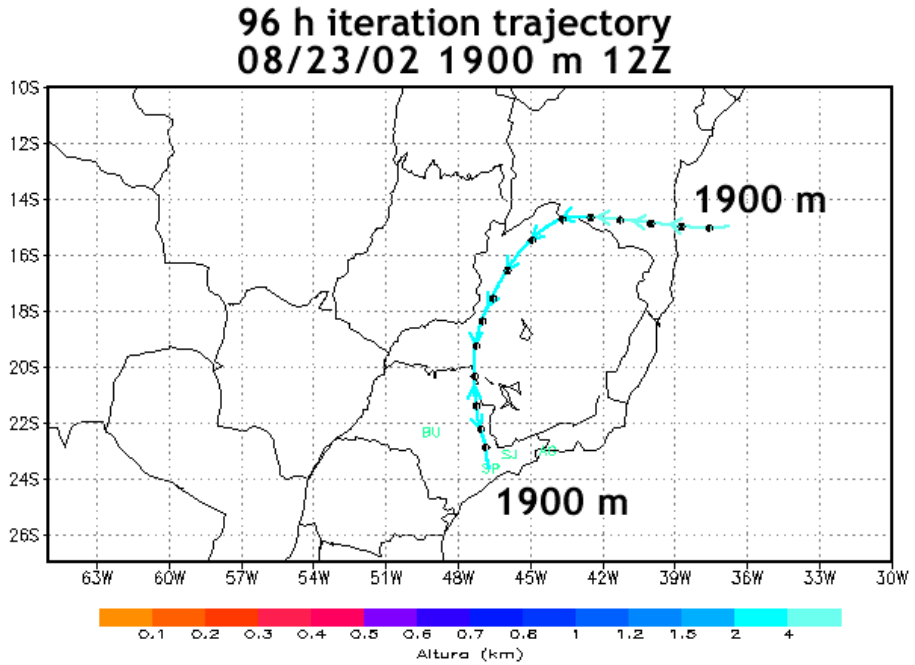

Fig. 17. 3D 96-hours air mass back-trajectory analysis for air masses ending over São Paulo, Brazil, on 23 August 2002 at 12:00 GMT at 1900 m.

ACPD
3, 2835–2877, 2003

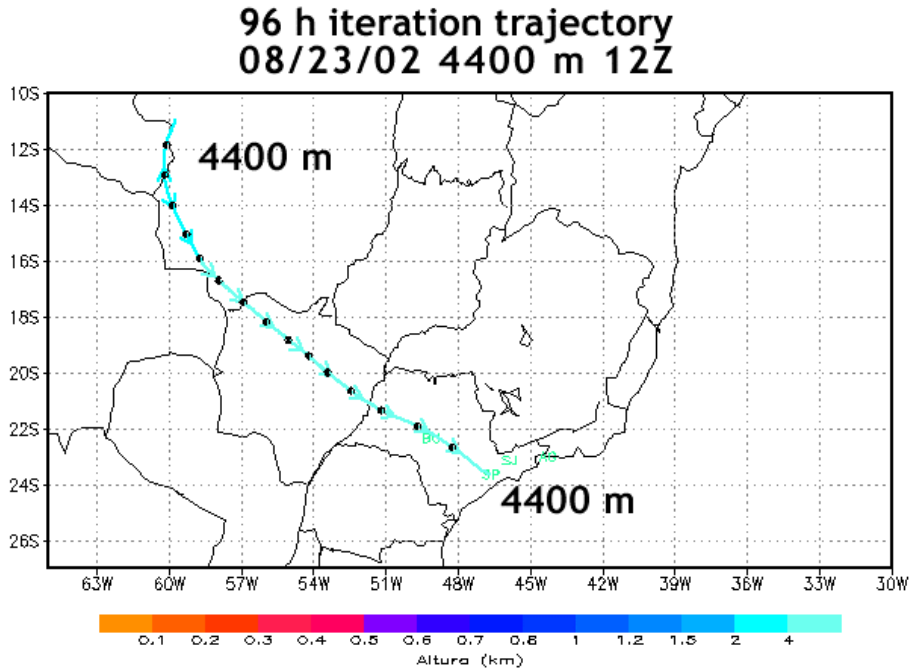

Fig. 18. 3D 96-hours air mass back-trajectory analysis for air masses ending over São Paulo, Brazil, on 23 August 2001 at 12:00 GMT at 4400 m.

ACPD
3, 2835–2877, 2003

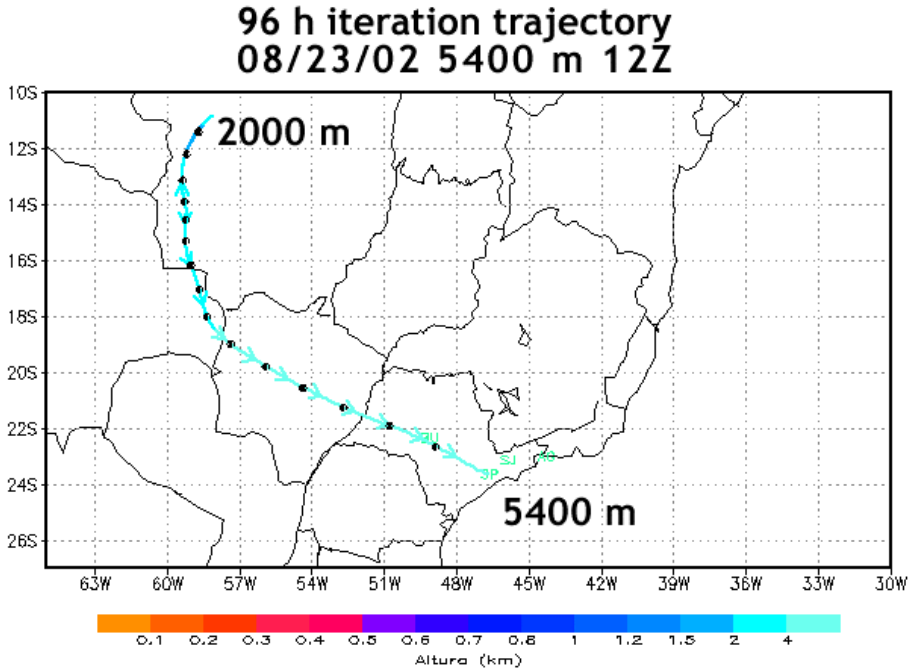

Fig. 19. 3D 96-hours air mass back-trajectory analysis for air masses ending over São Paulo, Brazil, on 23 August 2001 at 12:00 GMT at 5400 m.

ACPD
3, 2835–2877, 2003

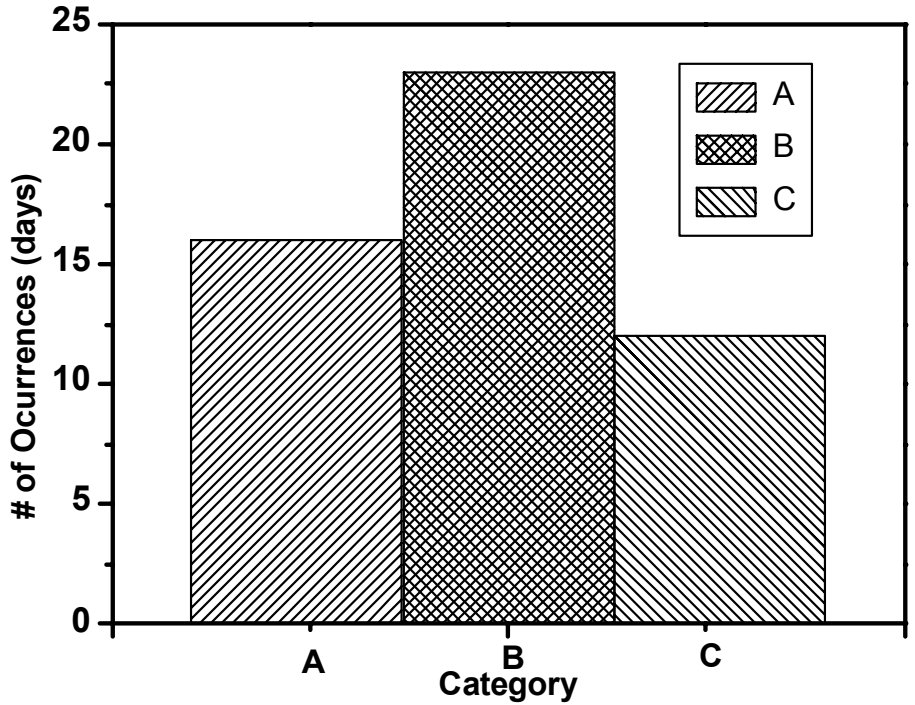

Fig. 20. Histrogram showing the frequency of Categories A, B and C for the LIDAR measurements.

ACPD
3, 2835–2877, 2003